

Structure and disorder of phosphates in $\text{Ag}_2\text{O-AgI-P}_2\text{O}_5$ glasses

J. W. Zwanziger, K. K. Olsen, and S. L. Tagg

Department of Chemistry, Indiana University, Bloomington, Indiana 47405

(Received 24 February 1993)

We directly probe the microstructure of the different phosphates in several glasses in the $\text{Ag}_2\text{O-AgI-P}_2\text{O}_5$ system, by means of variable angle correlation NMR spectroscopy. This two-dimensional experiment separates the chemical-shift powder patterns of the phosphorus sites according to their isotropic chemical shifts. We have thus determined all chemical-shift tensor elements for each chemically distinct phosphorus site in these glasses, and their variation within each site. Our results yield a precise description of the phosphate types and geometries in these glasses.

Silver phosphate doped with silver iodide forms glasses with exceptionally high ionic conductivity at certain compositions.¹ Ionic conductors of this general type, consisting of a glass former, a network modifier, and a doping salt (here P_2O_5 , Ag_2O , and AgI , respectively) are promising for industrial applications, due to their electronic properties and ease of fabrication. However, discovering the mechanism of ionic conduction and the related problem of finding the relationship between the glass structure and the ion mobility have proven to be difficult tasks (see Ref. 2 and references therein). The temperature and frequency dependent dynamics of the silver iodide-silver phosphate system have been studied with a wide variety of methods.^{3,4} The structure of the glass matrix has been investigated as well,⁵⁻⁷ as has the interaction of the salt with the glass.⁸⁻¹⁰ These investigations have shown that the silver iodide does not greatly modify the network glass structure, and that the network itself consists of a variety of different phosphates.

As part of an effort to determine precisely how the mobile silver cations interact with the phosphate glass and the silver iodide, we have studied the microstructure of the phosphate sites using a recently developed NMR method.¹¹ The experiment, variable angle correlation spectroscopy (VACSYS), separates the anisotropic chemical-shift powder patterns according to the isotropic chemical shifts, using a second spectral dimension. We are thus able to characterize unambiguously the different phosphate units in these glasses. Additionally, we can investigate the chemical shift changes within the disorder-broadened peaks arising from different phosphate types, and from them determine quantitatively the different bonding geometries that exist in the glass.¹² We have thus arrived at a much more detailed description of the glassy matrix in these ionic conductors than was previously possible. Our results show as well that this method has great potential for revealing structural details in other disordered systems.

In this paper we discuss three compositions: $(\text{Ag}_2\text{O})_{41}(\text{AgI})_{39}(\text{P}_2\text{O}_5)_{20}$ (sample 1); $(\text{Ag}_2\text{O})_{35}(\text{AgI})_{44}(\text{P}_2\text{O}_5)_{21}$ (sample 2); and $(\text{Ag}_2\text{O})_{12}(\text{AgI})_{44}(\text{P}_2\text{O}_5)_{14}$ (sample 3). These compositions were chosen as representative of the different local phosphate structures attributed to this system.⁷ The samples were prepared by heating weighed amounts of AgNO_3 , AgI , and $(\text{NH}_4)_2\text{HPO}_4$ together in a porcelain

crucible over a Bunsen burner. The molten samples were heated for an additional 20 min after cessation of gas evolution, and quenched by pouring onto a stainless steel plate. The samples were crushed to powders in order to perform sample-spinning NMR experiments; all sample handling was carried out in a darkroom. The powdered samples were checked for crystallinity with powder x-ray diffraction—sample 3 was partially crystalline, the others were amorphous, in agreement with previous work on these compositions.⁷

All NMR spectra were acquired at 80.99 MHz under ambient conditions. The VACSYS experiment has been described in detail by Frydman *et al.*¹¹ Briefly, it utilizes the fact that for isolated spin-1/2 nuclei under fast sample spinning conditions, the contribution of the anisotropic part of the chemical shift to the evolution scales with $P_2(\cos\beta)$, where β is the angle between the sample spinning axis and the applied magnetic field and P_2 is the second Legendre polynomial. A set of free-induction decays (FID's) recorded at different spinning angles is used to interpolate onto the points of a square lattice, constructed such that one time dimension includes only evolution due to the isotropic part of the shift tensor, and the other dimension, only the anisotropic part. For the VACSYS spectra in this paper, 32 sample spinning angles were used, covering the range $-0.48 \leq P_2(\cos\beta) \leq 0.48$. The sample spinning frequency was typically 7 kHz. The 32 FID's, each consisting of 512 complex points, were phased and normalized to their first points, interpolated onto a 512×512 array, smoothed with an exponential decay of 5 ppm spectral width, and Fourier transformed. The spectra are displayed in magnitude mode.

Figure 1(a) shows the VACSYS spectrum of sample 1, along with one-dimensional spectra of the sample under static [Fig. 1(b)] and magic angle spinning (MAS) conditions [Fig. 1(c)]. The MAS spectrum shows two peaks, indicating that this sample contains two types of phosphate groups. The powder patterns due to these groups overlap in the static spectrum, and it would be difficult to deconvolute that pattern into its components, especially since each component is broadened by the disorder in the glass (detectable in the MAS spectrum, though in a highly averaged way). In contrast, in the VACSYS spectrum one clearly sees the separation of the powder patterns arising from the different phosphorus sites. The

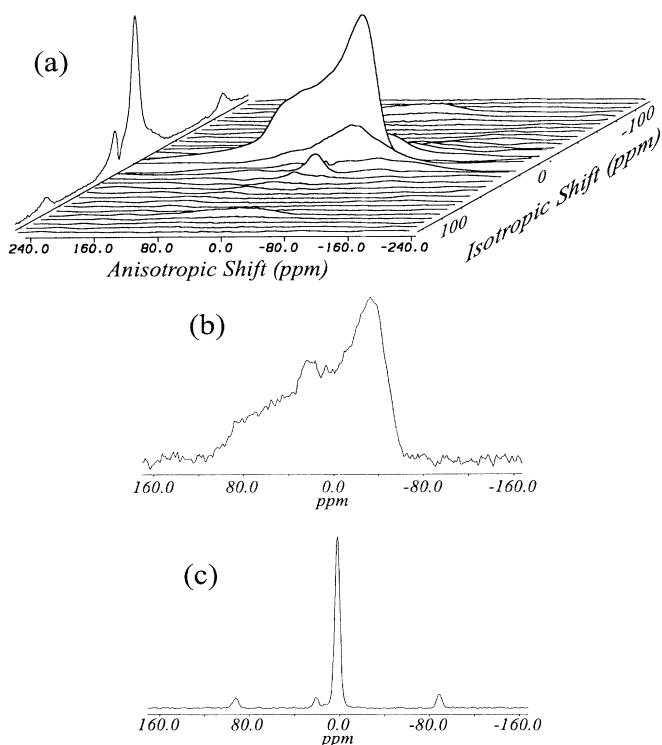


FIG. 1. (a) P-31 VACS Y NMR spectrum of $(\text{Ag}_2\text{O})_{41}(\text{AgI})_{39}(\text{P}_2\text{O}_5)_{20}$ (sample 1), with the projection on the isotropic axis at the left edge; (b) static P-31 NMR spectrum of sample 1; (c) magic angle spinning P-31 NMR spectrum of sample 1; the peaks at ± 90 ppm are spinning sidebands. Here and throughout the paper, chemical shifts are reported relative to 85% aqueous H_3PO_4 .

width and shape of the contours of the VACS Y spectra [Figs. 2(a) and 3(a)] contain information about the disorder within each site. We display these variations by showing slices through the spectra at different isotropic shifts [Figs. 2(b)–2(d) and 3(b)–3(d)]. The chemical-shift data are summarized in Table I. The uncertainties reported there arise from several factors. These include residual dipolar coupling between the phosphorus atoms, smoothing of the data and presentation in magnitude mode, and the disorder of the glass. We estimate that in our experiments the residual dipolar coupling is no more than about 4 ppm, and generally less due to the scaling factor $P_2(\cos\beta)$. Due to the smoothing and the mode of data presentation, then, we consider changes in the tensor elements of more than 7–10 ppm as significant, and attribute them to changes in the local phosphorus environment.

Both the isotropic and anisotropic chemical-shift tensor elements of phosphorus in phosphates reflect the local electronic charge density around the phosphorus atom involved. Figure 4 shows typical phosphorus oxoanions and their characteristic chemical-shift powder patterns.¹³ The local symmetry of the phosphorus environment confers a characteristic shape on the associated powder pattern, which can include both anisotropy (positive or negative) and asymmetry.¹⁴ The isotropic chemical shifts of phosphorus in these glasses have been used to assign

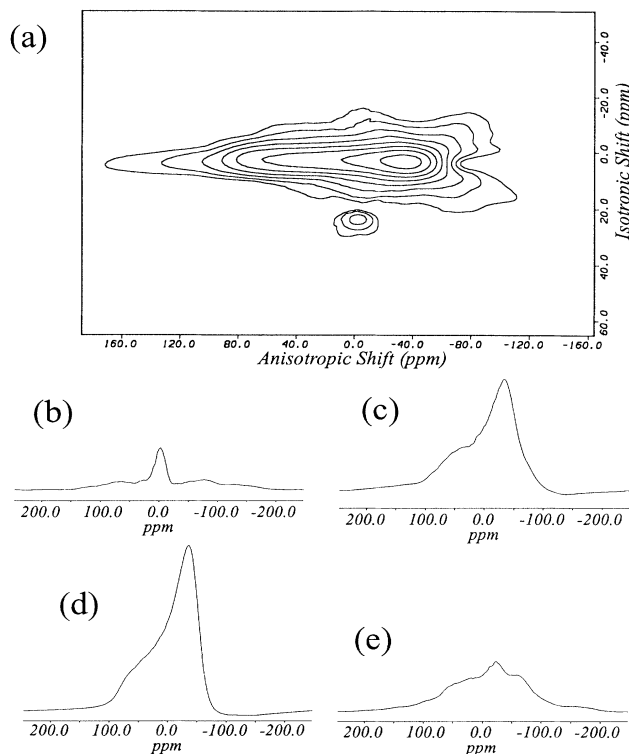


FIG. 2. (a) Contour plot of the P-31 VACS Y NMR spectrum of $(\text{Ag}_2\text{O})_{41}(\text{AgI})_{39}(\text{P}_2\text{O}_5)_{20}$ (sample 1); (b) slice through the VACS Y spectrum at isotropic shift 23.6 ppm; (c) the same, at 8.1 ppm; (d) same, at 3.3 ppm; (e) same, at -7.3 ppm. All slices are shown scaled to the intensity of slice (d).

the local chemical structure, by comparing the observed shifts to those in model compounds.⁷ That work suggested that peaks with isotropic shifts near 20 ppm are due to orthophosphate (PO_4^{3-}), those with shifts near 0 ppm, to pyrophosphate ($\text{P}_2\text{O}_7^{4-}$), and upfield shifts near -15 ppm, to nonterminal phosphates in polyphosphate.

The MAS spectrum of sample 1 shows a strong peak at 3.3 ppm, and a weak peak (5% as intense) at 23.6 ppm. With VACS Y, we can study the full powder pattern of each of these sites independently of the others. The slice at an isotropic shift of 3.3 ppm is shown in Fig. 2(d). The shape of the pattern shows a large positive anisotropy but no asymmetry. The anisotropic shift tensor elements can be obtained directly from the spectrum as 73 ± 7 ppm, -37 ± 7 ppm, and -37 ± 7 ppm. These values and the shape are typical of pyrophosphate [cf. Fig. 4(b)], as is the average isotropic shift for this site, thus confirming the earlier assignment⁷ of this resonance. The detailed structure of these pyrophosphates can be extracted by using the empirical correlation between anisotropy and bond length in POX_3 compounds.¹⁵ Using our measured chemical-shift tensor elements, we determine a distance of 1.7 Å between the phosphorus atom and the bridging oxygen. This length is characteristic of a phosphorus-oxygen single bond, from which one may conclude that

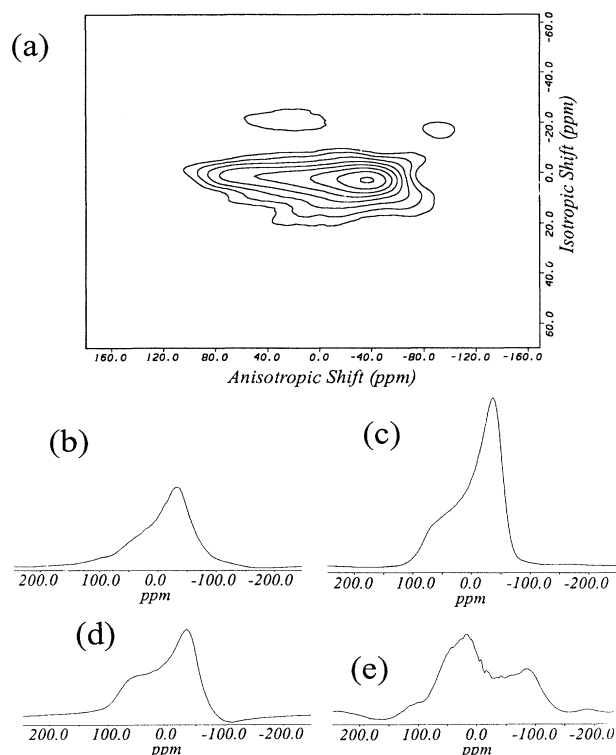


FIG. 3. (a) Contour plot of the P-31 VACSYS NMR spectrum of $(\text{Ag}_2\text{O})_{35}(\text{AgI})_{44}(\text{P}_2\text{O}_5)_{21}$ (sample 2); (b) slice through the VACSYS spectrum at isotropic shift 8.1 ppm; (c) same, at 3.3 ppm; (d) same, at -1.5 ppm; (e) same, at -20 ppm. The intensities are scaled to slice (c), except for (e), which is magnified by a factor of 2.

the excess charge in these pyrophosphate units is localized on the bonds to the terminal oxygen.

The pyrophosphate peak retains a residual width of several ppm due to the disorder in the glass. We can probe the nature of this disorder directly with the VACSYS experiment, as we show in Figs. 2(c)–2(e). There, slices at different isotropic shifts are shown, all within the pyrophosphate peak. We see from the slices that in fact the chemical shift tensor is different at different points in the resonance, changing from a shape

TABLE I. Chemical shift tensor elements as a function of isotropic chemical shift. Only the anisotropic parts of the shift tensor elements are reported, that is, $\sigma_{ii} - \sigma_{\text{iso}}$. All shifts are given in units of ppm, and the anisotropic elements have an uncertainty of ± 7 ppm.

Composition	Species	σ_{iso}	σ_{ZZ}	σ_{XX}	σ_{YY}
$(\text{Ag}_2\text{O})_{41}(\text{AgI})_{39}(\text{P}_2\text{O}_5)_{20}$ (sample 1)	ortho	23.6	0	0	0
	pyro	8.1	58	-34	-34
		3.3	73	-37	-37
$(\text{Ag}_2\text{O})_{35}(\text{AgI})_{44}(\text{P}_2\text{O}_5)_{21}$ (sample 2)	pyro	-7.3	74	-67	-22
		8.1	47	-33	-33
		3.3	71	-37	-37
$(\text{Ag}_2\text{O})_{12}(\text{AgI})_{44}(\text{P}_2\text{O}_5)_{14}$ (sample 3)	ortho	-1.5	66	-33	-33
		21.7	0	0	0
	pyro	3.3	70	-40	-40

typical of pyrophosphate, with zero asymmetry, at an isotropic shift of 8.1 ppm [Fig. 2(c)], to a different shape, with nonzero asymmetry $\eta = 0.6 \pm 0.1$, at a point shifted upfield to -7.3 ppm [Fig. 2(e)]. The downfield slice [Fig. 2(c)] has a smaller anisotropy than the slice at the isotropic average, discussed above. This reduction in anisotropy suggests a shortening of the bond to the bridging oxygen and an increase in π -bond character¹⁵—in other words, the phosphates of these pyrophosphate units are more symmetrical, thus resembling orthophosphate (for which the P-O bond order is 1.5). This interpretation is in accord with the fact that this slice is on the upfield edge of the peak (that is, shifted towards the usual location of orthophosphate). The appearance of nonzero asymmetry in the upfield part of the pyrophosphate peak suggests that in a portion of the pyrophosphate units the local C_{3v} symmetry has been distorted, though the positive, rather than negative, anisotropy indicates that it is not distorted so much as in the polyphosphate fragments. Furthermore, the upfield shift of the isotropic frequency suggests that in these fragments the net charge localized near the phosphorus has been reduced. We thus hypothesize that these phosphates have near-neighbor cations which are nearer to one or two of the three nonbridging oxygen atoms of the phosphate. Such a cation might be Ag^+ in AgI. We are currently performing this experiment on Ag-109 in order to investigate such a possibility.

Figure 2(b) shows a slice through the VACSYS spectrum of sample 1, at an isotropic shift of 23.6 ppm. This shift corresponds to the maximum of the smaller peak

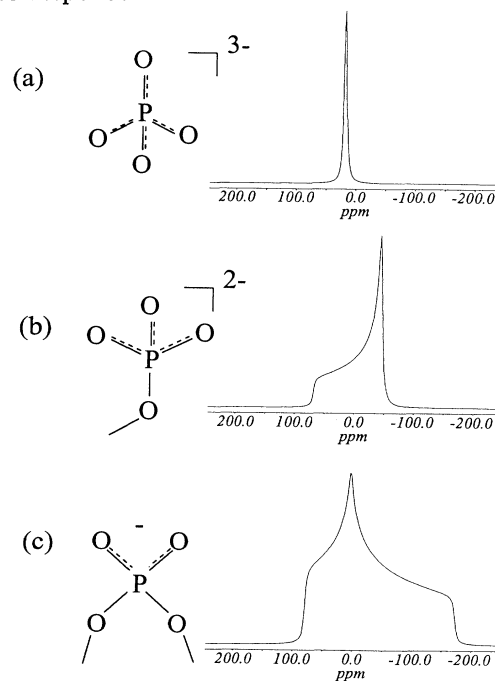


FIG. 4. Structure and typical powder pattern for phosphorus in (a) an orthophosphate unit, PO_4^{3-} , showing neither anisotropy nor asymmetry; (b) pyrophosphate, $\text{P}_2\text{O}_7^{4-}$, showing positive anisotropy and zero asymmetry; and (c) a nonterminal phosphate in polyphosphate, showing negative anisotropy and nonzero asymmetry.

in the MAS spectrum. The powder pattern has tensor elements $\sigma_{ii} - \sigma_{\text{iso}} = 0 \pm 7$ ppm, $i = X, Y, Z$. From the symmetric shape we conclude that the phosphorus site from which it arises is of locally tetrahedral symmetry, and that fact, combined with the isotropic shift, confirms the assignment of the site to orthophosphate. Especially for a relatively weak site such as this, it is significant that we obtain the line shape with no interference from neighboring sites.

In sample 2 the proportion of network modifier (Ag_2O) is reduced, compared to sample 1. The MAS spectrum shows again a peak at 3.3 ppm, and a weaker peak (10% as intense) at -20 ppm. Figure 3 shows the VACSYS spectrum of sample 2. Again, slices at isotropic shift values allow us to assign the anisotropic chemical shift tensor values for each type of site. In this sample there is again the pyrophosphate structure, at an average isotropic shift of 3.3 ppm [Fig. 3(c)]. The anisotropy again suggests that the bond to the bridging oxygen is a single bond. Additionally, the downfield slice [Fig. 3(b)] shows a small reduction in anisotropy and consequently bond length. The upfield slice [Fig. 3(d)], in contrast to sample 1, shows no asymmetric character, but rather resembles the other pyrophosphate units. In sample 2 there is additionally a small peak at an isotropic shift of -20 ppm. This peak has been previously assigned to nonterminal phosphate in polyphosphate chains, by correlating upfield shifts with reduction in charge localized near the phosphorus.⁷ We can see from VACSYS [Fig. 3(e)] that the powder pattern of the upfield site shows substantial asymmetry ($\eta = 0.4 \pm 0.1$) and a negative anisotropy, both of which are signatures of nonterminal phosphate in polyphosphate [Fig. 4(c)]. These direct observations render the assignment unambiguous. In the static spectrum the powder pattern for this site is unobservable, since it is covered by the broad, more intense pattern of the pyrophosphate. Finally, in this sample we see no indication of orthophosphate, in accord with the reduction in network modifier concentration.

In sample 3 the proportion of glass former (P_2O_5) is reduced, and this sample is partially crystalline. Our VACSYS results yield a narrow powder pattern at an isotropic shift of 21.7 ppm, which we assign to orthophosphate based on the line shape and shift. We see addition-

ally a weak (10% as intense) isotropic peak at 3.3 ppm, the powder pattern of which is typical of pyrophosphate. The tensor elements (Table I) show that these units are similar to those found at 3.3 ppm in the other compositions. From the line shapes it appears that the phosphate in the glassy portion of the sample does not take conformations grossly different from that in the crystalline portion.

To summarize, we have studied the phosphate microstructure in several glasses in the Ag_2O - AgI - P_2O_5 system with the two-dimensional NMR experiment VACSYS. The advantage of this experiment is that it separates the anisotropic chemical-shift powder patterns according to their isotropic shifts, thus permitting study of the structural variations within a chemical species. Our results substantially extend the general picture of the structure of these glasses. Based on the shapes of the powder patterns, we have determined the different types of phosphate units present, finding chain phosphates (pyrophosphate and polyphosphate) at low network modifier concentration, and increasing orthophosphate concentration as the proportion of network modifier to glass former is increased. We have also directly probed the disorder within the pyrophosphate in our glassy samples, finding that it can contain a fraction distorted from local C_{3v} symmetry, and with less net charge, and also a portion with more nearly equivalent bonds, approaching tetrahedral symmetry. We are currently working to extend these results to include estimates of bond angles in the phosphates, and to use the relative intensities to extract site populations in the different local environments within each chemical type. We are also applying this method to the silver nuclei, to complete the picture of the structure and its influence on the dynamics.

It is a pleasure to thank Professor L. Frydman and Professor S. Martin for helpful discussions, and Amoco Research Corporation for donation of an NMR spectrometer. Acknowledgment is made to the Donors of The Petroleum Research Fund, administered by the American Chemical Society, for partial support of this research; this material is based upon work supported by the National Science Foundation under Grant No. DMR-9115787.

¹ T. Minami, Y. Takuma, and M. Tanaka, *J. Electrochem. Soc.* **124**, 1659 (1977).

² C. A. Angell, *Annu. Rev. Phys. Chem.* **43**, 693 (1992).

³ S. W. Martin, *Mater. Chem. Phys.* **23**, 225 (1989).

⁴ C. A. Angell, *Chem. Rev.* **90**, 523 (1990).

⁵ T. Minami, T. Katsuda, and M. Tanaka, *J. Phys. Chem.* **83**, 1306 (1979).

⁶ J. P. Malugani and R. Mercier, *Solid State Ionics* **13**, 293 (1984).

⁷ S. Hayashi and K. Hayamizu, *J. Solid State Chem.* **80**, 195 (1989).

⁸ M. Tachez, R. Mercier, J. P. Malugani, and P. Chieux, *Solid State Ionics* **25**, 263 (1987).

⁹ A. Musinu, G. Piccaluga, and G. Pinna, *J. Chem. Phys.* **89**, 1074 (1988).

¹⁰ L. Borjesson, L. M. Torell, V. Dahlborg, and W. S. Howells, *Phys. Rev. B* **39**, 3404 (1987).

¹¹ L. Frydman, G. C. Chingas, Y. K. Lee, P. J. Grandinetti, M. A. Eastman, G. A. Barrall, and A. Pines, *J. Chem. Phys.* **97**, 4800 (1992).

¹² Separation of interactions has been profitably exploited to study silicate glasses, using dynamic angle spinning NMR to probe the quadrupole interactions of oxygen-17 nuclei. See I. Farnan, P. J. Grandinetti, J. H. Baltisberger, J. F. Stebbins, U. Werner, M. A. Eastman, and A. Pines, *Nature* **358**, 31 (1992).

¹³ H. Eckert, *Prog. NMR Spectrosc.* **24**, 159 (1992).

¹⁴ We label the three principal elements of the chemical-shift anisotropy according to $|\sigma_{zz}| \geq |\sigma_{xx}| \geq |\sigma_{yy}|$. For the anisotropy we take $\sigma_{zz} - (\sigma_{xx} + \sigma_{yy})/2$, and for the asymmetry $(\sigma_{yy} - \sigma_{xx})/\sigma_{zz}$. Note that the isotropic component has been removed from our reported shift tensor elements.

¹⁵ A.-R. Grimmer, *Spectrochim. Acta* **34A**, 941 (1978).